

# 3D Visualisation of Diffusion Flame Structure and Dynamics under Acoustic Excitation

Qian Wang<sup>a</sup>, Yang Zhang<sup>a</sup>, Hao Jie Tang<sup>b</sup>, Min Zhu<sup>b</sup>

<sup>a</sup> Department of Mechanical Engineering, University of Sheffield, Sheffield, S1 3JD, UK

<sup>b</sup> Key Laboratory for Thermal Science and Power Engineering, Department of Thermal Engineering, Tsinghua University, Beijing, 100084, China

## 1 Introduction

Laminar gas jet diffusion flames have been intensively studied in combustion science. The understanding of diffusion flame stabilization mechanisms is essential for industrial applications, such as engine and furnace designs, safety consideration, costs cutting, combustion efficiency improvement and pollutant emissions reduction. It is found that laminar jet diffusion flames show a typical phenomenon of flickering/oscillating at a low frequency of 10-20 Hz [1]. In a flickering flame, the flame and flow interactions show periodic and reproducible characteristics. It was found that the flame oscillation frequency is correlated with the large toroidal vortex structures outside the visible flame zone due to buoyancy-driven instability [2-4]. Buckmaster et al. [5] employed a linear instability theory and showed that the flame buoyancy could result in a modified Kelvin-Helmholtz type instability.

In addition to the natural buoyant induced vortex oscillation, flame behaviours can be significantly altered by applying external acoustic excitation. Acoustically excited flame has been studied intensively because it has the advantage to control the flame oscillation at specific frequencies and therefore it is convenient to synchronise with measurement devices. Depending on the frequency and magnitude, the addition of forced acoustic field can produce considerable modification to the dynamic flame structure and movement [6]. The use of external acoustic perturbation also has an effect on combustion at chemical-level, thus resulting in the change of emissions [7], various molecular concentrations and consequently the perceptual flame colouration [8]. Furthermore, for a practical burner or combustor with high noise levels, the acoustic perturbation sources may cause serious combustion instability phenomena [9]. Therefore, the understanding of the detail physical insight of the acoustic excited combustion process is of great importance.

During this investigation, it was found that under some conditions the flame flickering frequency became locked at precisely one-half the excitation frequency for a wide range of forcing conditions. Subharmonic flame response in pulsed buoyant diffusion flames has been reported in a laminar slot burner flame with air-side forcing [10] and in transitional jet flames with fuel pulsing [11]. The 2D subharmonic flame structures were interrogated through the use of laser diagnostics [12]. In another experimental apparatus, when the fuel (methane and propane) is mixed, the diffusion flame shows half the peak frequency of that of the pure fuel [13]. The local flame structure is of great help to gain physical insights into the combustion process. However, the flame structure is irregular and can't be well understood by only 2D images. The main focus of this paper is to investigate the global 3D flame structure and dynamics by high speed stereo imaging techniques. The results give improved phenomenological insight into the nature of the buoyant instability under acoustic excitation and should provide definitive experimental data for comparison with detailed modeling studies.

Stereoscopic, or 3D photography, works because human brain is able to recreate the illusion of depth with two images at slightly different directions. Modern industry and research hires stereoscopic technology to detect and record 3D information based on projective geometry. The depth information can be reconstructed from two images through camera calibration and corresponding points extracted

from the two images. In this study, a stereo adapter is attached to the front of the high speed camera lens to record the stereo image pairs. The stereo adapter consists of four delicate flat mirrors and could form two images at slightly different angles on the camera focus plane. The 3D surface could be reconstructed and observed based on the camera calibration and reconstruction technique established by Zhang [14], which provides the depth information in quantitative. The implementation of modern high-speed camera is advantageous to provide temporal resolution to determine the time-dependent flame structure behaviour under different combustion and acoustic excitation conditions.

## 2 Experimental setup

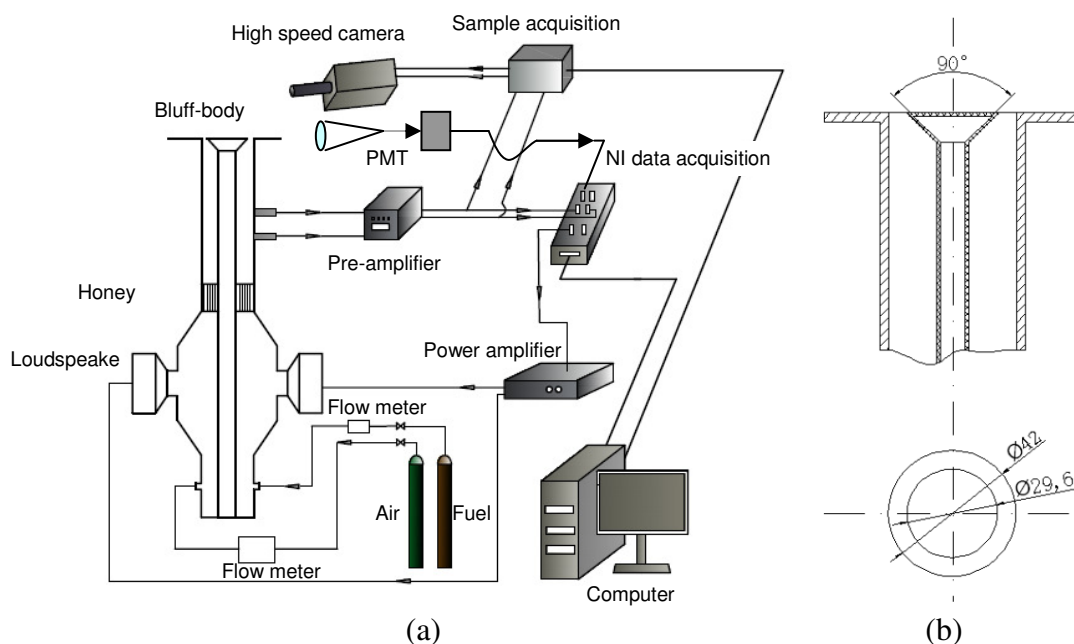


Figure 1. (a) Schematic of the experimental setup; (b) Dimension of the bluff body

The schematic layout of the experimental apparatuses is illustrated in Figure 1(a). The burner utilised in this study is designed to establish a wide range of diffusion and premixed bluff-body stabilised flames. Gaseous fuel and air can be supplied from separate cylinders and controlled by dedicated flowmeters. The range of flow for air and fuel is 0-500 slpm (standard litre per minute) and 0-50 slpm respectively. Gaseous reactant stream enters the mixing chamber from the lower-end of the combustor. A honeycomb section is located above the mixing chamber, which straightens the flow along the burner length towards the nozzle-exit. The flame is established at the nozzle which is stabilised by a conical bluff-body structure (shown in Figure 1(b)) at the combustor exit. The outer diameter of the nozzle exit is 42mm with the conical bluff-body diameter of 29.6mm, thus giving a blockage ratio 0.5. In this investigation, methane diffusion flame at volumetric fuel flow rate of 5slpm was considered, and no air was supplied to the combustor. External acoustic excitation was provided by two loudspeakers which are forced by a power amplifier whose amplitude and frequencies could be controlled as desired. These speakers generate periodic pressure oscillation which modulates the diffusion flame burning characteristics at the burner exit. In the current experiment, the flame characteristics under acoustic excitation frequency range of 6-20Hz were investigated. The burner design also incorporates pressure detection points along the length of the vertical burner pipe (see Figure 1). Two microphones were placed at different points (see Figure 1) to detect the pressure oscillation. A photomultiplier (PMT) is applied to record the flame flickering frequency based on the flame light emissions. The dynamic flame behaviours under acoustic excitation field were captured by a high speed camera with a stereo adapter attached in front of the lens. The framing rate is set at 1,000 fps, which is sufficient to get time resolved stereo image pairs for the frequency analysis and 3D

structure reconstruction. The high speed imaging and acoustic pressure measurement and PMT flame signals are synchronized for tractable analysis. A z-type schlieren setup with a pair of parabolic mirrors is used to observe the vortex development with a view field of 150 mm.

### 3 Results and discussion

Table 1: Selected case conditions

Case No.	$f_e$ (Hz)	$A_e$ (pa)	$f_m$ (Hz)
Case 1	8	1.1	8
Case 2	8	3.5	4

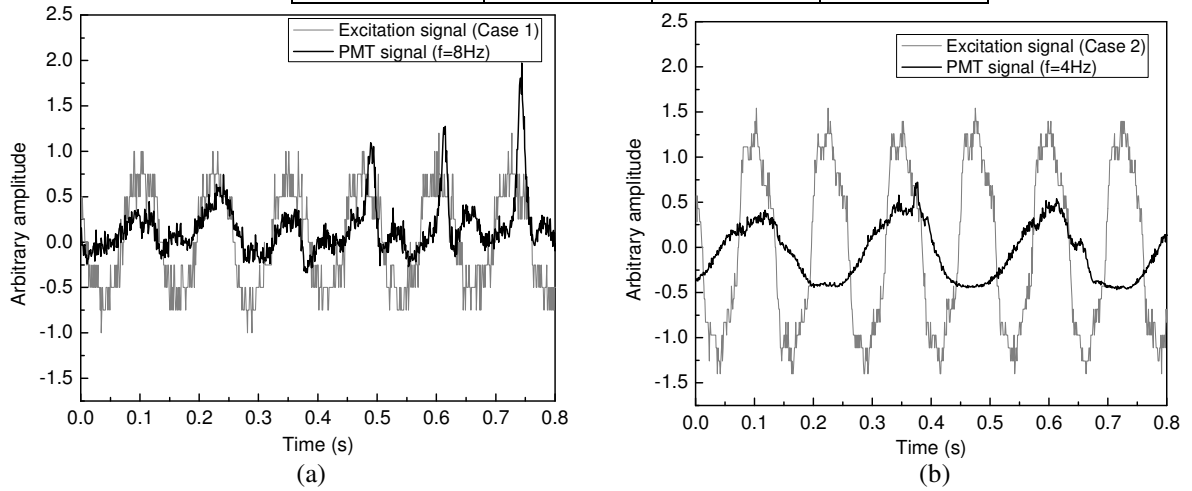


Figure 2. Acoustic excitation and PMT signal (a) Case 1; (b) Case 2

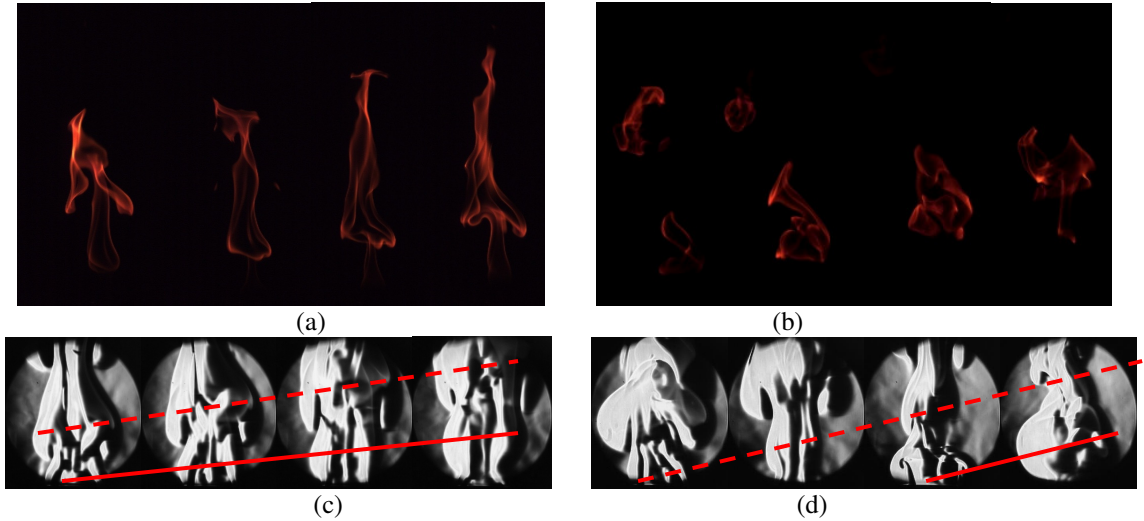


Figure 3. Flame image sequence at 0, 90, 180 and 270 degree (a) Case 1; (b) Case2  
Schlieren image sequence at 0, 90, 180 and 270 degree (c) Case 1; (d) Case 2  
(Dash line: upper vortex evolution; Solid line: lower vortex evolution)

The natural flame flickering frequency is evaluated by the PMT signal and the value is 7.5 Hz. For consistency, we designate  $f_m$  as the dominant flame flickering frequency,  $f_e$  the acoustic excitation frequency and  $A_e$  the acoustic excitation amplitude. When the acoustic excitation is applied to the flame, the frequency changes with the increasing amplitude of the excitation signal. In this work it was also discovered that acoustic excitation at low frequency would first shift the dominant frequency from the buoyancy driven flickering frequency to the excitation frequency and then the half excitation

frequency if the excitation intensity level was increased further. The appearance of half frequency indicates the nonlinear response of the flame oscillation to the external forcing function. In the frequency range of 6 Hz to 20 Hz investigated in this study, a half frequency is observed in each case. As noted in the introduction, such characteristics have not been reported in most previous studies on the modulated buoyant diffusion flames. Since the diffusion flame itself is turbulent in local structure, the 3D structure of the flame is worthy of exploration to gain physical insights. In order to investigate the acoustic excitation effect on flame structure, two typical cases are selected for 3D structure comparison. The case conditions are listed in Table 1. Case 1 is the buoyant diffusion flame modulated at the excitation frequency. Since the excitation frequency is close to the natural flame flickering frequency, the flame and vortex shape is similar but more regular compared to the case without excitation. Case 2 is a typical sample flame oscillating at half excitation frequency.

The acoustic and PMT signals of the two cases are shown in Figure 2. For Case 1, the PMT signal shows the same time period with the excitation pressure signal. For Case 2, the period of the PMT signal is double of the acoustic excitation signal, which indicates the flame frequency is half the excitation frequency. For each case, four images are selected to display the cycle characteristics based on the phase degree of the flickering period. The selected four phase degrees are illustrated in Figure 3. The 2D flame and vortex structures are shown in Figure 3 by high speed direct and schlieren images. The four images correspond to the phase degree of 0, 90, 180 and 270 from left to right respectively. All the images are taken at 1,000 fps. Since the dominant frequency of Case 2 is half of that of Case 1, the time interval in the image sequence of Case 2 is double that of Case 1 as well. From the direct 2D image of Case 1 shown in Figure 3 (a), a triangle-shaped flame is formed from an initial apex shape from the exit of the nozzle. In contrast, the 2D flame structure of Case 2 is shorter and wider with a tortuous shape. The vortex evolutions of the two cases are illustrated in Figure 3 (c-d). In Case 1, the vortices are formed evenly from the exit of the nozzle and shedding in the downstream direction one by one. The vortex size is similar in the following two vortices. In Case 2, the initiation frequency of the vortex at the nozzle exit is the same as that of Case 1. However, the vortex size is different for every two neighbouring vortices. As shown in Figure 3 (d), the lower vortex (highlighted by solid line) is much bigger than the upper one. In the last image, only a much bigger vortex could be observed, which indicates that the smaller vortex is merged by the following bigger vortex in the process of shedding in the downstream direction. It could be concluded that the acoustic excitation affected the vortex evolution process and thus change the flame flickering frequency.

The 3D structures of the two cases are reconstructed based on the calibration parameters and the correspondence point coordinates. The correspondence points are obtained through an area based correlation algorithm. Although only the bright part flame with textures could be reconstructed, it may still provides useful information to evaluate the 3D structure of the flame. The raw data reconstructed are only clouds of point coordinates in 3D space. The flame surface is represented by the 3D mesh grid method. The reconstructed flame structures are visualised at three different view angles in Figure 4 and Figure 5 respectively. The view angle in the first image of each group is the same as the 2D image taken by the camera. It could be observed that most part of the flame structures are reconstructed and the principle features are presented. The similarity of the reconstructed image and the original 2D image shows the reasonable accuracy of the stereoscopic reconstruction. The images at different view angles show clearly the flame distribution in 3D space. The very different perception when viewed at different view angles demonstrates the necessity of 3D visualisation. The flame of Case 1 has a long and narrow structure and shows a slightly helical trend along the downstream direction. In contrast, the half frequency flame of Case 2 is shorter with obvious tortuous shape biased in one side in 3D space. The flame shape in both cases corresponds well with the direct 2D flame images shown Figure 3(a-b). The dramatic change in the 3D flame structure must be caused by the strong pressure perturbation induced by the acoustic excitation. On the one hand, the fuel/air mixing and combustion process is influenced by the acoustic wave. On the other hand, the coupling between

the buoyancy and the excitation induces the vortex evolution change and thus affects the flame structure consequently.

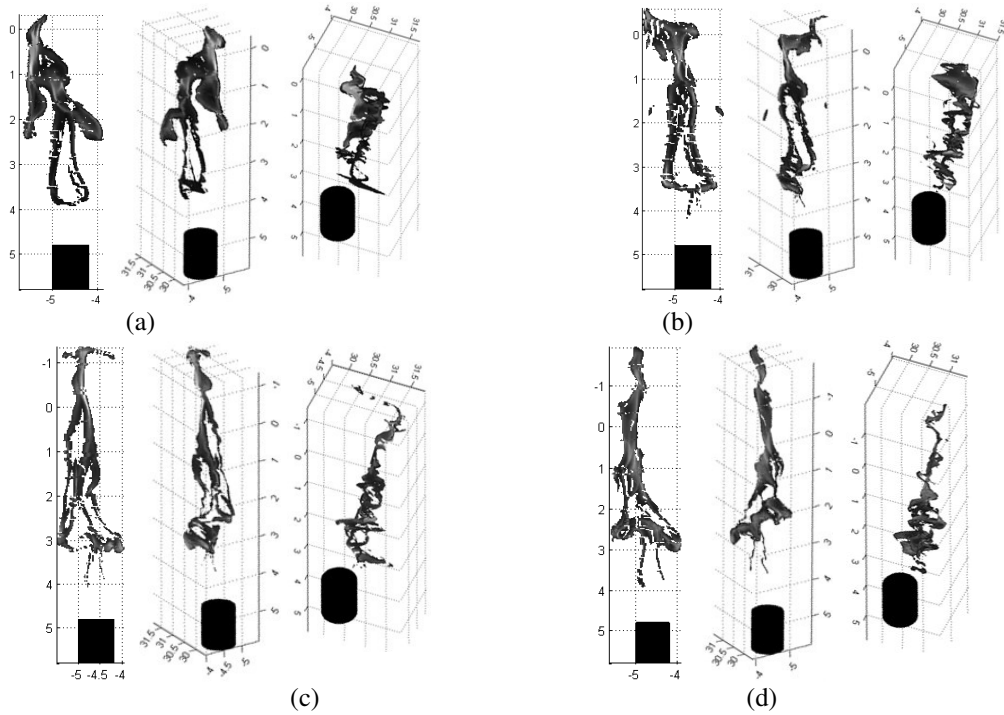


Figure 4. Reconstructed 3D flame structure at different view angles of Case 1 at phase angle (a) 0; (b) 90; (c) 180; (d) 270 degree

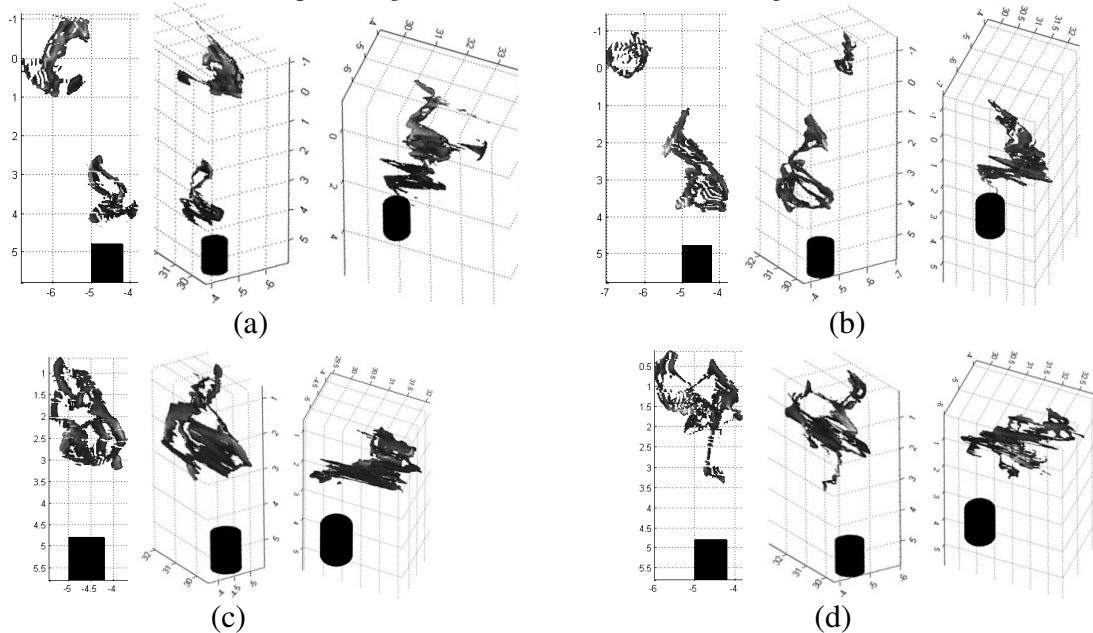


Figure 5. Reconstructed 3D flame structure at different view angles of case 2 at phase angle (a) 0; (b) 90; (c) 180; (d) 270 degree

## 4 Conclusions

In this paper, the acoustic modulated methane diffusion flame dynamics are investigated using high speed schlieren and stereo imaging techniques. It is found that the flame is able to stabilise either at the same or half the excitation frequencies when the excitation frequency is set at specific amplitudes.

Two typical cases under 8 Hz excitation but different amplitudes are analyzed for the comparison of both the flame structure and vortex evolution process. The flame is oscillating at the excitation frequency in one case and half the excitation frequency in the other. The high speed schlieren images show that the initiation vortex frequencies are the same from the nozzle exit. However, a bigger vortex merges the smaller one and shedding in the downstream direction in the half frequency case. The acoustic induced pressure fluctuation influence on the vortex evolution causes the double period of the flame flickering cycle. The 3D structures of the flame in two cases are reconstructed based on the stereo reconstruction method and show dramatic differences in 3D shape.

## Acknowledgement

Q. Wang would like to thank the University of Manchester, the University of Sheffield and BP Alternative Energy International Ltd for providing PhD scholarships during which part of this research work was carried out. This research is further supported by EPSRC through the Grant No. EP/G063044/1 and the Chinese State Bureau of Overseas Experts.

## References

- [1] Buckmaster J and Peters N. (1988). The infinite candle and its stability-A paradigm for flickering diffusion flames. *Proc. Combust.* 21: 1829.
- [2] Chamberlin D S and Rose A. (1948). The flicker of luminous flames *Proc. Combust.* 1-2: 27.
- [3] Farhat S A, Ng W B and Zhang Y. (2005). Chemiluminescent emission measurement of a diffusion flame jet in a loudspeaker induced standing wave. *Fuel.* 84: 1760.
- [4] Katta V R and Roquemore W M. (1993). Role of inner and outer structures in transitional jet diffusion flame. *Combust.Flame.* 92: 274.
- [5] Kim K T, Lee J G, Quay B D and Santavicca D A. (2010). Response of partially premixed flames to acoustic velocity and equivalence ratio perturbations. *Combust. Flame.* 157: 1731.
- [6] Kimura I. (1965) Stability of laminar-jet flames. *Proc. Combust.* 10: 1295.
- [7] Li J and Zhang Y. (2010). Fuel mixing effect on the flickering of jet diffusion flames. *Proc. IME C J. Mech. Eng. Sci.* DOI: 10.1243/09544062JMES2258.
- [8] Rocha A M A, Carvalho Jr J A and Lacava P T. (2008). Gas concentration and temperature in acoustically excited Delft turbulent jet flames. *Fuel.* 87:3433.
- [9] Saito M, Sato M and Nishimura A. (1998). Soot suppression by acoustic oscillated combustion *Fuel.* 77: 973.
- [10] Stocker D P S, J.C.; Chen, L. D. 1993 Preliminary Observations of the Effect of Microgravity on a Pulsed Jet Diffusion Flame Fall Meeting of the Western States Sec.The Combustion Inst. Paper 93-065.
- [11] Thuillard M. (2002). A new flame detector using the latest research on flames and fuzzy-wavelet algorithms. *Fire Safety J.* 37: 371.
- [12] Timothy C. Williams C R S, Rober W. Schefer, Pascale Desgroux. (2007). The response of buoyant laminar diffusion flames to low-frequency forcing. *Combust Flame.* 151: 676.
- [13] Toong T Y, Richard F S, John M S and Griffin Y A. (1965). Mechanisms of combustion instability. *Pro. Combust.* 10: 1301.
- [14] Zhang Z. (2000). A flexible new technique for camera calibration. *IEEE TPAMI.* 22: 1330.